Supplementary Information (SI)

Local cargo delivery to double bilayer compartments

Rui Liu, ‡[a] Ruslan Ryskulov, ‡[a] Esteban Pedrueza-Villalmanzo, [a] Irep Gözen [b] and Aldo Jesorka *[a,b]

[a] Department of Chemistry and Chemical Engineering, Chalmers University of Technology, 41296, Göteborg, Sweden

[b] GOMOD AB, Göteborg, Sweden

‡Authors contributed equally, *Correspondent author: aldo.jesorka@gomod.eu

1. Fabrication

SI Fig.1 contains several fabrication-related additional details concerning solutions to process-related problems and flow rate measurements. Panel **A** points to a recurrent problem of resist artefacts around the edges of the long narrow tip, likely arising from third layer laminate folding down during the roll lamination step. Panel **B** shows the improved design with a 40 µm resin-free frame (arrow) around the entire device. Panel **C** is a magnification of the tip region of the device after development. This image also reveals significant crack formation in the sharp corners of the frame around the device tip, even though slow cooling in the PEB step was applied. This is not of concern as it does not involve the device structures. As a general design consideration, well known to be important for conventional SU-8 resist processing, sharp corners should be avoided in all device features.

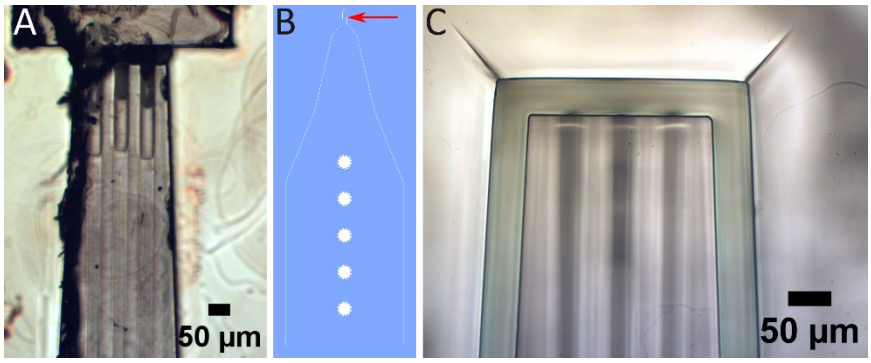

SI Figure 1. Device fabrication-related details. A Micrograph of a device tip with a single support pillar at a distance of 30 µm from the tip (after development). **B** Screenshot of the engineering scheme produces in AutoCAD of the 40 µm narrow gap placed around the periphery of the device to prevent folding of the top laminate layer, eliminating the artefacts shown in **A**. The amount of viscous resin/developer mixture that can enter the channel is very much reduced and alleviates plug formation considerably. **C** Micrograph of the tip region according to the design shown in **B**.

2. Device interface

For deployment, the fabricated open space microfluidic device was attached to a holder featuring solution and waste wells, using double sided transfer tape shaped to the device footprint with a Cricut Explore 3 cutting plotter. A schematic drawing of the 3D printed holder and a photograph of the deployed device are shown in **SI Fig.2**.

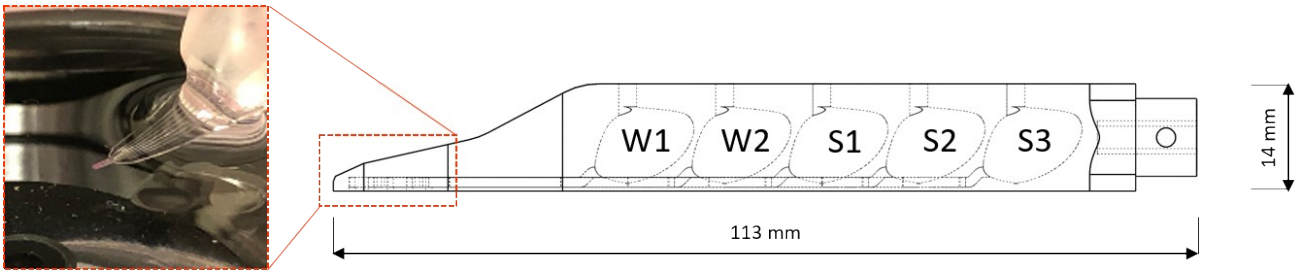

SI Figure 2: Holder interface for microfluidic device. Schematic drawing (section) of the holder with three solution (S1-S3) and two waste reservoirs (W1, W2), according to the designations in manuscript **Fig. 2**. The inset is a photograph of the deployed device in an open volume on an inverted research microscope table. The 3D model was generated with the SolidWorks package, converted to STL format and sliced in the Formlabs software. The supply channel dimensions are 1 x 1 mm; these channels do not contribute to the flow rates of the laminated chip device. They can be considered an extension to the reservoirs.

3. Rupture and Encapsulation

This section contains data and analyses for additional transformation/encapsulation experiments. Two examples and a fluorescence intensity analysis are provided for each of the two cases: completely de-wetted DBL with surface-exposing fractures (**SI Fig.3-5**), and for conventional transformations with distal bilayer fractures only (**SI Fig.6-8**).

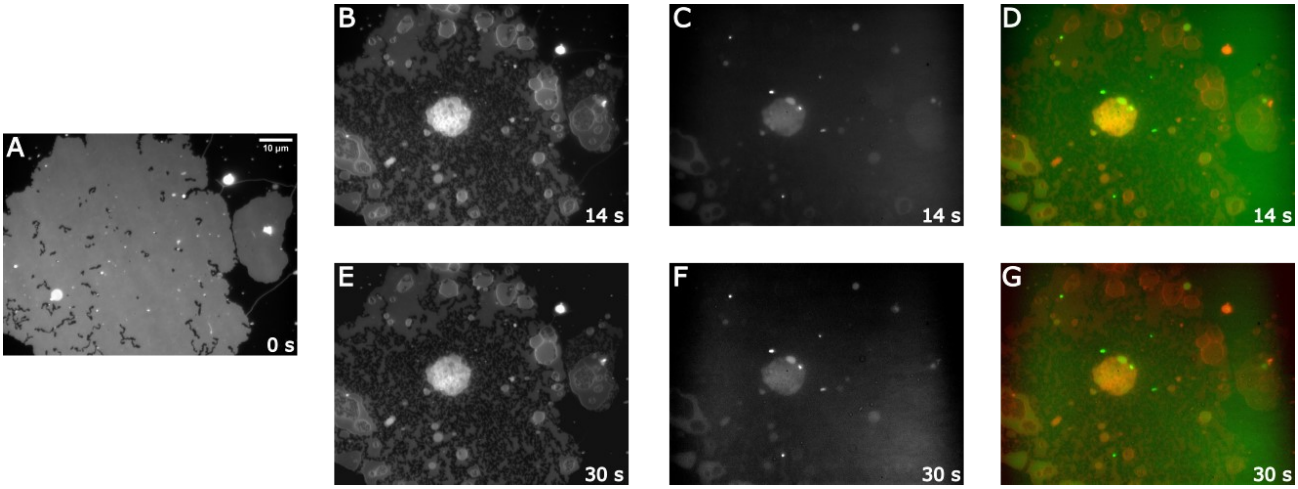

SI Figure 3: Retention of encapsulated cargo - additional example 1. Encapsulation example featuring a membrane patch completely de-wetted DBL, i.e. Fractures in the DBL which expose the surface. **A** Membrane patch before heat-initiated transformation (0 s). **B-D** Membrane, cargo and combined channel fluorescence micrographs at 14 s after superfusion. **E-G** Membrane, cargo and combined channel fluorescence micrographs at 30 s after superfusion.

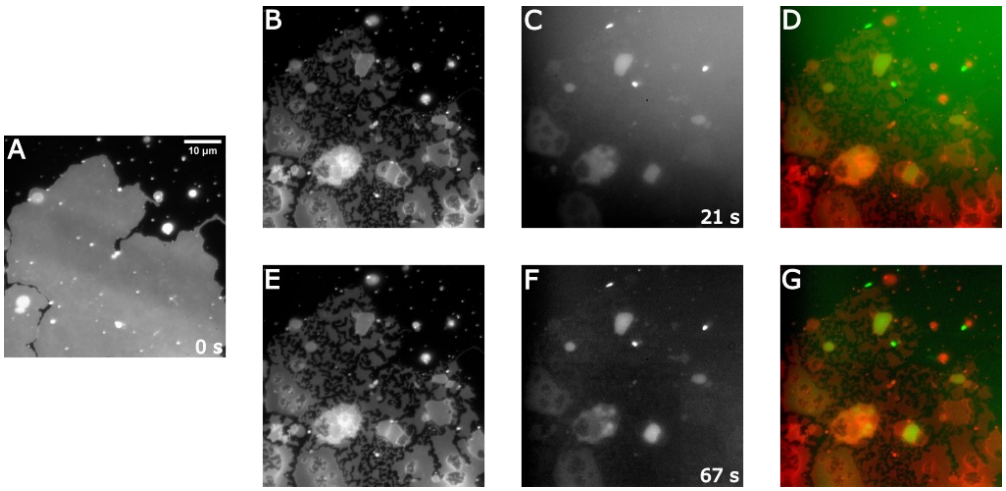

SI Figure 4: Retention of encapsulated cargo - additional example 2. Encapsulation featuring a membrane patch completely de-wetted DBL, i.e. Fractures in the DBL which expose the surface. **A** Membrane patch before heat-initiated transformation (0 s). **B-D** Membrane, cargo and combined channel fluorescence micrographs at 21 s after superfusion. **E-G** Membrane, cargo and combined channel fluorescence micrographs at 67 s after superfusion.

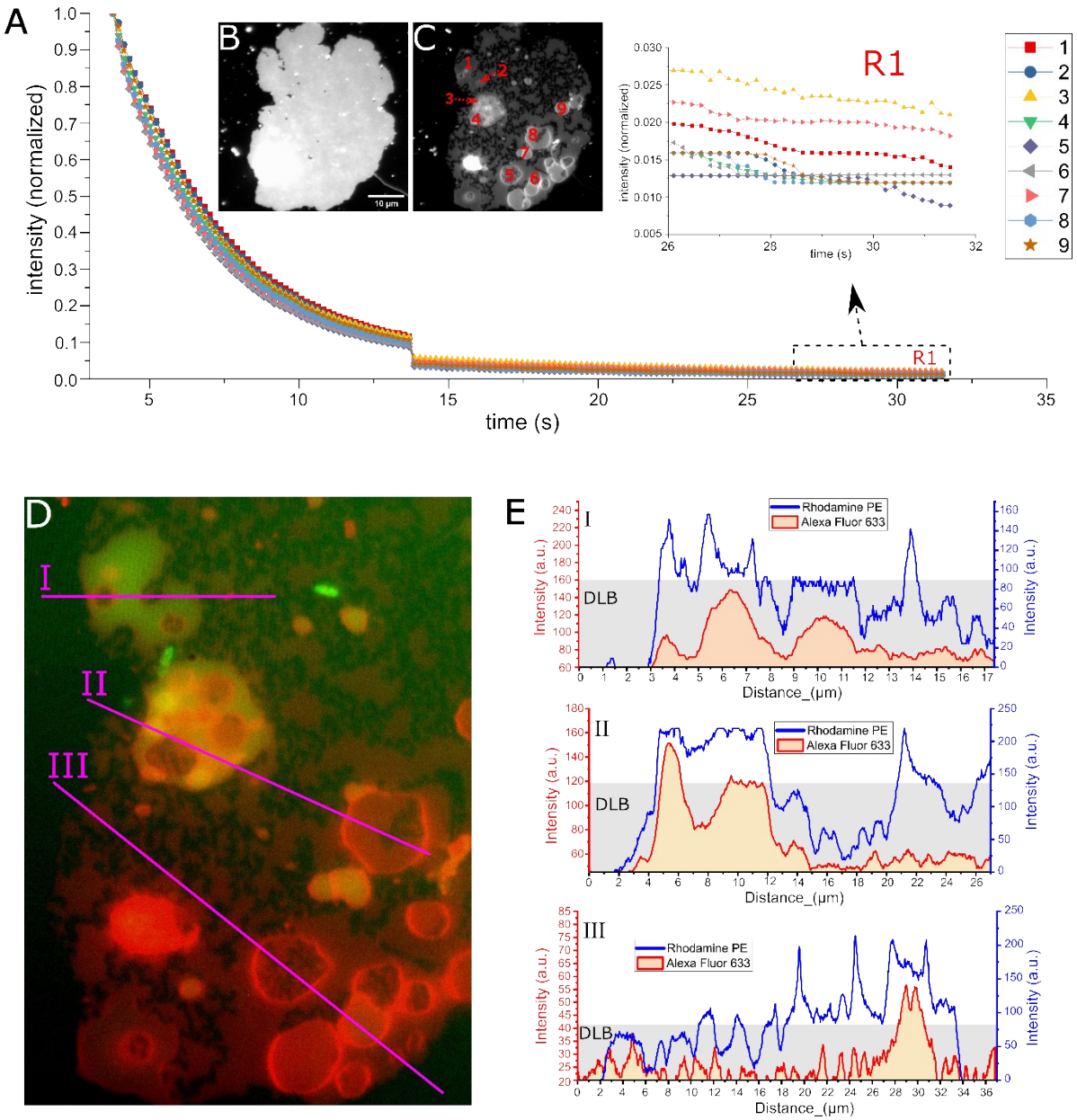

SI Figure 5: Heat-induced transformations of double lipid bilayer membrane patches - additional example 3. Time development of cargo fluorescence in different areas on transformed membrane patches. A Development of fluorescence intensity over time in nine regions of interest after heat-induced shape transformation under encapsulation of externally supplied fluorescent Alexa Fluor 633 dye solution. The abrupt drop in the fluorescence intensity of the plots is due to two consecutive video recordings. Panel **B-C** arranged as an inset to **A**, are micrographs taken of the membrane patch before (B) and after (C, t=44.72 s) the IR laser exposure and encapsulation (fluorescence signal: membrane label). **R1** A magnified region of graph **A**. **D** Transformed membrane patch shown in **B**, magenta lines I, II and III are intensity profiles corresponding to **E**.

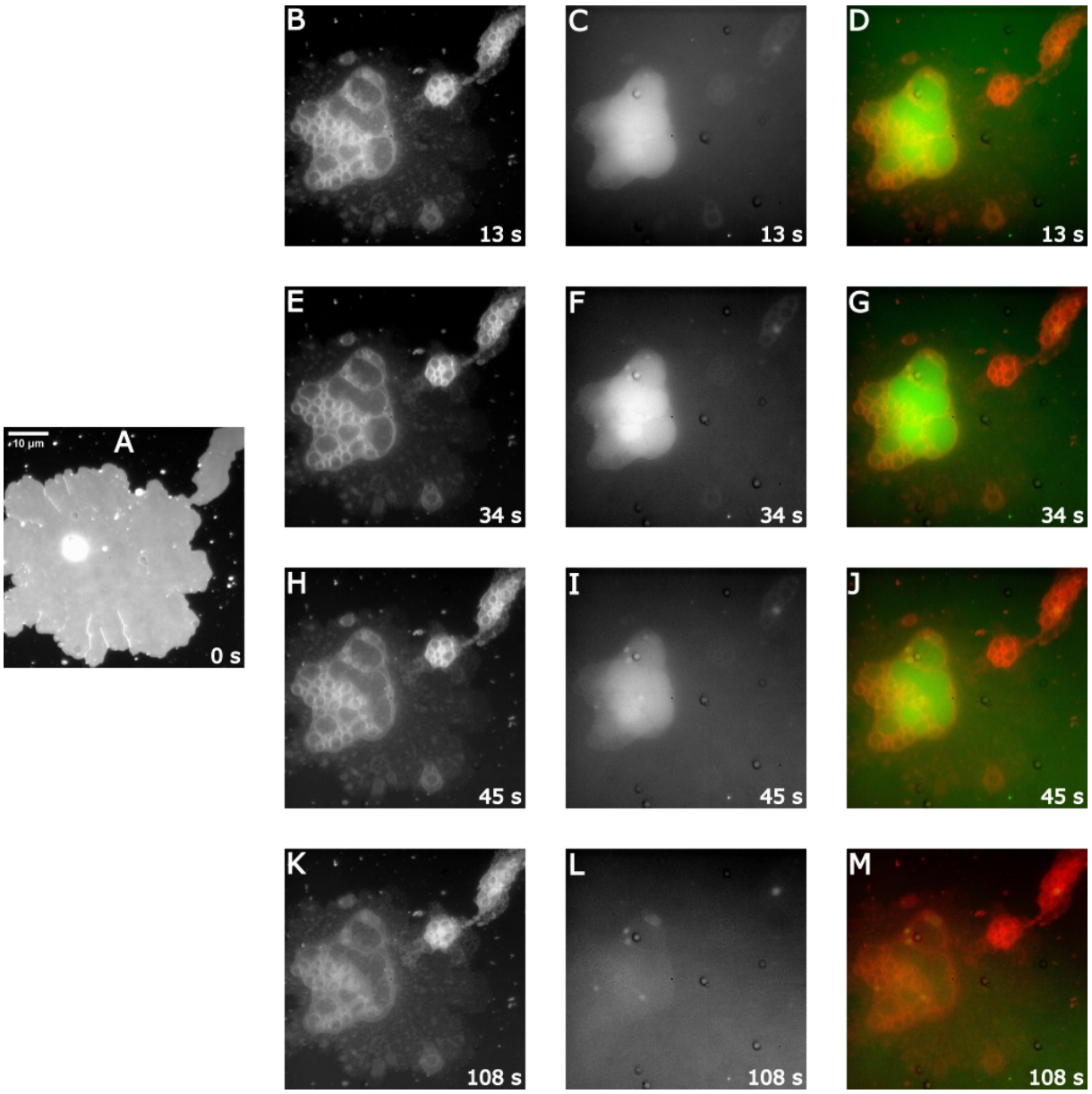

SI Figure 6: Retention of encapsulated cargo - additional example 4. Encapsulation featuring a membrane patch with conventional de-wetting of the distal bilayer, where the surface remains covered by the proximal bilayer. **A** Membrane patch before heat-initiated transformation (0s). **B-D**, **E-G**, **H-J** and **K-M** represent membrane, cargo and combined channel fluorescence micrographs at 13, 34, 45 and 108 s after superfusion, respectively.

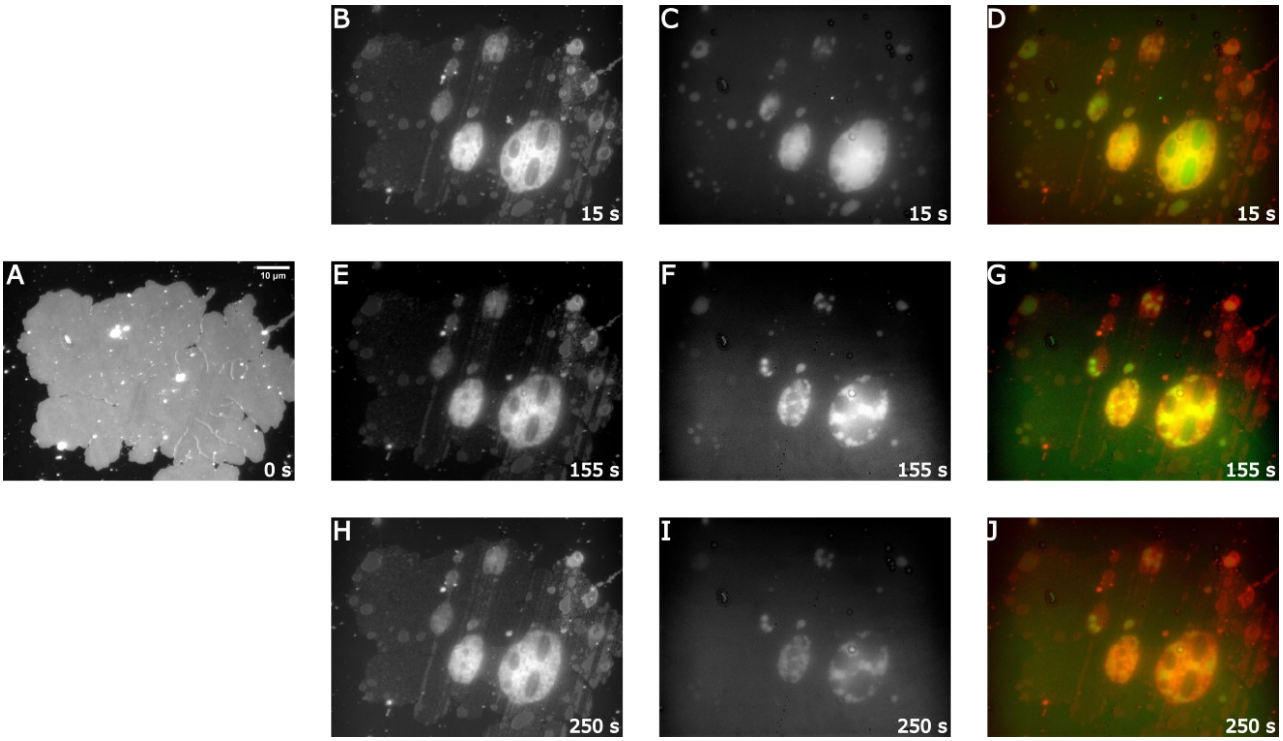

SI Figure 7: Retention of encapsulated cargo - additional example 5. Encapsulation featuring a membrane patch with conventional de-wetting of the distal bilayer, where the surface remains covered by the proximal bilayer. **A** Membrane patch before heat-initiated transformation (0s). **B-D**, **E-G** and **H-J** represent membrane, cargo and combined channel fluorescence micrographs at 15, 155 and 215 s after superfusion, respectively.

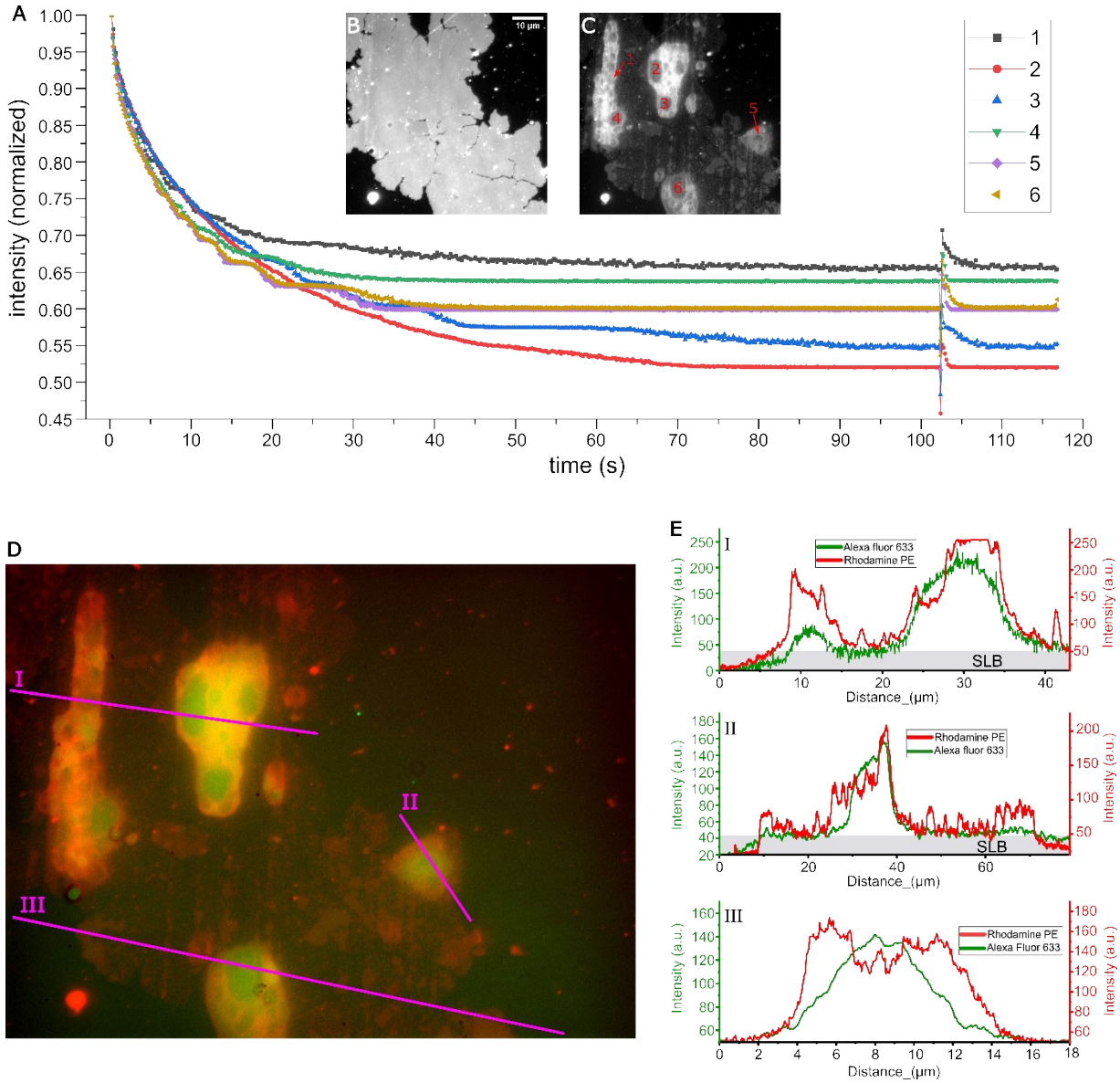

SI Figure 8: Heat-induced transformations of double lipid bilayer membrane patches - additional example 6. Time development of cargo fluorescence in different areas on transformed membrane patches. A Development of fluorescence intensity over time in six regions of interest after heat-induced shape transformation under encapsulation of externally supplied fluorescent Alexa Fluor 633 dye solution. The sudden intensity increase (~103 s.) is due to a slight camera gain adjustment. The Panels **B-C** arranged as an inset to **A**, are micrographs taken of the membrane patch before (B) and after (C, t=126.24 s) the IR laser exposure and encapsulation (fluorescence signal: membrane label). **D** Transformed membrane patch shown in **B**. Magenta lines I, II and III are intensity profiles corresponding to **E**.

SI Video 1: Solution switching in the microfluidic device(10x).
SI Video 2: Confinement at the tip of the microfluidic device(10x).
SI Video 3: Example 1 of the fluorescent cargo encapsulation (100x).
SI Video 4: Example 2 of the fluorescent cargo encapsulation (100x).
SI Video 5: Example 3 of the fluorescent cargo encapsulation (100x).
SI Video 6: Example 4 of the fluorescent cargo encapsulation (100x).
SI Video 7: Example 5 of the fluorescent cargo encapsulation (100x).
SI video 8: Video recording of the experiment shown in Figure 4 of the main article.